第 35 卷第 9 期
2019 年 9 月

无 机 化 学 学 报
CHINESE JOURNAL OF INORGANIC CHEMISTRY

Vol.35 No.9
1651-1658

席夫碱类混价七核锰金属配合物的合成、表征及磁性

杨立国*,[1] 王 芳[1] 耿翠环[1] 余智超[1] 王 鑫[1]
王 凯[1] 张永辉[1] 牛永生[1] 李大成[2]
([1]安阳工学院化学与环境工程学院,安阳 455000)
([2]聊城大学化学化工学院,聊城 252000)

摘要:以 3-乙氧基水杨醛缩乙醇胺席夫碱(H_2L)为配体合成了 2 个新的七核锰配合物$[Na_2Mn^{Ⅱ}Mn^{Ⅲ}_6O_2(L)_6(N_3)_4(CH_3COO)_2]\cdot 4DMF$ (**1**)和$[Na_2Mn^{Ⅱ}Mn^{Ⅲ}_6O_2(L)_6(SCN)_4(CH_3COO)_2]\cdot 2DMF$ (**2**),并对它们进行红外分析、元素分析、热重分析和单晶结构分析。单晶衍射结果表明,配合物 **1** 和 **2** 均为混价七核锰配合物,包含 1 个 Mn^{2+}和 6 个 Mn^{3+}。此外还研究了配合物 **1** 和 **2** 的磁学性质,磁性研究表明配合物 **1** 和 **2** 都表现出反铁磁作用。

关键词:锰;席夫碱;晶体结构;磁学性质
中图分类号:O614.71+1 **文献标识码**:A **文章编号**:1001-4861(2019)09-1651-08
DOI:10.11862/CJIC.2019.164

Heptanuclear Manganese Complexes with Schiff-Base Ligand: Syntheses, Crystal Structures and Magnetic Properties

YANG Li-Guo*,[1] WANG Fang[1] GENG Cui-Huan[1] YU Zhi-Chao[1] WANG Xin[1]
WANG Kai[1] ZHANG Yong-Hui[1] NIU Yong-Sheng[1] LI Da-Cheng[2]
([1]*College of Chemistry and Environmental Engineering, Anyang Institute of Technology, Anyang, Henan* 455000, *China*)
([2]*School of Chemistry and Chemical Engineering, Liaocheng University, Liaocheng, Shandong* 252000, *China*)

Abstract: Two new mixed-valence heptanuclear manganese complexes, $[Na_2Mn^{Ⅱ}Mn^{Ⅲ}_6O_2(L)_6(N_3)_4(CH_3COO)_2]\cdot 4DMF$ (**1**) and $[Na_2Mn^{Ⅱ}Mn^{Ⅲ}_6O_2(L)_6(SCN)_4(CH_3COO)_2]\cdot 2DMF$ (**2**) (H_2L=3-ethoxy-6-(((2-hydroxyethyl)imino)methyl) phenol), were synthesized by treating the Schiff-base ligand with $Mn(OAc)_2\cdot 4H_2O$, and characterized by elemental analysis, IR spectra, thermogravimetric analyses and X-ray single crystal diffraction. X-ray single crystal diffraction analysis reveals that **1** and **2** have a similar new mixed-valence heptanuclear structure. The magnetic measurements indicate that **1** and **2** exhibit the antiferromagnetic interactions. CCDC: 1849331 **1**; 1849333, **2**.

Keywords: manganese; Schiff base; crystal structures; magnetic properties

0 Introduction

Polynuclear manganese complexes are attracting considerable attention in several different fields ranging from bioinorganic chemistry to solid-state physics [1]. Low-nuclearity species have been extensively studied as models for the water oxidizing complex in photosystem Ⅱ [2], whereas nanometer-size clusters with high-spin ground states are currently being investigated as single-molecule magnets[3]. From a synthetic point

收稿日期:2019-03-25。收修改稿日期:2019-05-06。
河南省高等学校重点科研项目(No.18A150020)和安阳市化学生物传感重点实验室基金(No.21302003)资助。
*通信联系人。E-mail:lgyang@ayit.edu.cn,Tel:15670010482。

of view, chemists have learned to exploit hydrolytic reactions, which naturally lead to insoluble metal oxides and oxohydroxides as final products. By proper use of suitable organic ligands, mainly carboxylates[4], polyamines[5], and polyols[6], the "growth" of the metal cores can be controlled in such a way to obtained finite-size clusters. Some ligands have been used to synthesize the manganese complexes, such as triethanolamine[7], salicylaldoxime[8], Alkoxide ligands[9], dipyridyl ketone[10]. Due to the effect of ligand fields and different coordination modes, the complexes will excite different magnetic properties. To our best of knowledge, the Schiff-base ligand, 3-ethoxy-6-(((2-hydroxyethyl)imino)methyl) phenol (H_2L), has not been used to synthesized the manganese complexes.

To further study the interaction between the ligand and the property, two new manganese complexes, $[Na_2Mn^{Ⅱ}Mn^{Ⅲ}_6O_2(L)_6(N_3)_4(CH_3COO)_2]\cdot 4DMF$ (**1**) and $[Na_2Mn^{Ⅱ}Mn^{Ⅲ}_6O_2(L)_6(SCN)_4(CH_3COO)_2]\cdot 2DMF$ (**2**), have been synthesized by treating H_2L with $Mn(OAc)_2\cdot 4H_2O$ and characterized by elemental analysis, IR spectra and X-ray single crystal diffraction. The magnetic behavior of **1** and **2** indicates an antiferro-magnetic interaction between the Mn^{2+} and Mn^{3+} ions.

1 Experimental

1.1 Chemicals and general instruments

3-ethoxy-6-(((2-hydroxyethyl)imino)methyl phenol was prepared according to the published procedures[11]. All other reagents and solvents were used as received.

Thermogravimetric analysis (TGA) experiments were carried out on a NETZSCH STA 449F3 thermal analyzer from 40 to 800 ℃ under N_2 at a heating rate of 10 ℃·min^{-1}. Powder X-ray diffraction (PXRD) determinations was performed on an X-ray diffractometer (D/max 2500 PC, Rigaku) with Cu $K\alpha$ radiation (λ=0.154 06 nm). The crushed single crystalline powder samples were scanned at 40 kV (generator voltage) and 40 mA (tube current) from 5° to 50° with a step of 0.1°·s^{-1}. Elemental analyses were performed on an Elementar Vario MICRO CUBE elemental analyzer. The magnetic measurements were performed on SQUID-VSM.

1.2 Synthesis of $[Na_2Mn^{Ⅱ}Mn^{Ⅲ}_6O_2(L)_6(N_3)_4(CH_3COO)_2]\cdot 4DMF$ (1)

$Mn(OAc)_2\cdot 4H_2O$ (171.5 mg, 0.7 mmol), NaN_3 (13.0 mg, 0.2 mmol) and Schiff base ligand (H_2L) (125.4 mg, 0.6 mmol) were reacted in DMF (10 mL) in the presence of tetramethyl ammonium hydroxide. The solution was stirred for 5 hours at room temperature and filtered. The filtrate was left undisturbed to allow slow evaporation of the solvent. Black single crystals suitable for X-ray diffraction were obtained after a week. Yield: 73.1 mg, 32% (based on Mn). IR (KBr, cm^{-1}): 3 636(br), 2 362(s), 1 678(s), 1 602(m), 1 575(s), 1 526(s), 1 440(vs), 1 381(s), 1 357(w), 1 310(m), 1 234(m), 1 201(m), 1 116(vw), 1 034(vw), 971(vw), 831(w), 786(vw), 735(w), 650(w), 612(w). Anal. Calcd. for $C_{82}H_{112}Mn_7N_{22}Na_2O_{28}$(%): C, 43.07; H, 4.90; N, 13.48. Found(%): C, 43.12; H, 4.95; N, 13.42.

1.3 Synthesis of $[Na_2Mn^{Ⅱ}Mn^{Ⅲ}_6O_2(L)_6(SCN)_4(CH_3COO)_2]\cdot 2DMF$ (2)

The synthesis of **2** was same as that of **1** except that NaSCN (16.2 mg, 0.2 mmol) was used instead of NaN_3. Yield: 65.9 mg, 28% (based on Mn). IR (KBr, cm^{-1}): 3 652(br), 2 989(s), 1 602(s), 1 578(s), 1 524(vs), 1 440(s), 1 384(m), 1 312(m), 1 299(m), 1 183(vw), 1 116(vw), 1 029(w), 978(vw), 831(w), 755(w), 739(w), 659(w), 605(w). Anal. Calcd. for $C_{84}H_{110}Mn_7N_{14}Na_2O_{30}S_4$ (%): C, 42.81; H, 4.67; N, 8.32. Found (%): C, 42.78; H, 4.65; N, 8.26.

1.4 X-ray crystallography

Data were collected on a Bruker SMART APEX Ⅱ diffractometer equipped with a graphite-monochromatized Mo $K\alpha$ radiation (λ=0.071 073 nm) at room temperature by using an ω-2θ scan mode. The size of the crystal **1** and **2** are 0.18 mm×0.16 mm×0.10 mm and 0.28 mm×0.15 mm×0.12 mm, respectively. The raw data frames were integrated with SAINT$^+$, and the corrections were applied for Lorentz and polarization effects. There was no evidence of crystal decay during data collection in all cases. Absorption correction was applied by using the multi-scan program SADABS[12]. The structure was solved by direct methods, and all non-hydrogen atoms were refined anisotropically by least-squares methods on F^2 using the SHELXLS

program[13]. The aromatic H atoms were restrained to ride 0.093 nm from the relevant C atom, with U_{iso}(H)= 1.2U_{eq}(C), while the methyl H atoms were treated as rigid groups, pivoted about the attached C atom, with C-H bond lengths fixed at 0.096 nm and U_{iso}(H)= 1.5U_{eq}(C). The crystallographic data and structural refinement parameters are provide in Table 1. Selected bond lengths and angles of complexes **1** and **2** are listed in Table 2.

CCDC: 1849331, **1**; 1849333, **2**.

Table 1　Crystallographic data for complexes 1 and 2

Complex	1	2
Formula	$C_{82}H_{112}Mn_7N_{22}Na_2O_{28}$	$C_{84}H_{110}Mn_7N_{14}Na_2O_{30}S_4$
Formula weight	2 284.49	2 354.65
Crystal system	Monoclinic	Triclinic
Space group	$P2_1/c$	$P\bar{1}$
a / nm	1.339 80(5)	1.423 23(10)
b / nm	2.207 97(7)	1.433 10(10)
c / nm	3.348 29(8)	1.483 19(11)
α / (°)		70.956 0(10)
β / (°)	97.495(3)	77.596 0(10)
γ / (°)		71.369 0(10)
V / nm^3	9.820 4(5)	2.689 0(3)
Z	4	1
F(000)	2 904	1 213
D_c / (Mg·m^{-3})	1.545	1.454
μ / mm^{-1}	7.912	0.959
θ range / (°)	3.327~67.070	3.044~25.009
Reflection collected	33 369	39 762
Independent reflection	17 196 (R_{int}=0.070 3)	9 386 (R_{int}=0.033 2)
Parameter	1 293	645
R_1 [$I>2\sigma(I)$]	0.061 2	0.053 1
wR_2 [$I>2\sigma(I)$]	0.134 3	0.158 8
Goodness of fit	1.000	1.055

Table 2　Selected bond lengths (nm) and angles (°) for complexes 1 and 2

1					
Mn(1)-O(17)	0.188 1(3)	Mn(2)-O(20)	0.192 4(3)	Mn(6)-O(13)	0.220 8(4)
Mn(1)-O(16)	0.189 3(3)	Mn(2)-N(20)	0.199 4(4)	Mn(6)-N(11)	0.242 7(5)
Mn(1)-O(18)	0.192 6(3)	Mn(2)-O(25)	0.215 8(4)	Mn(6)-Mn(8)	0.316 18(12)
Mn(1)-N(22)	0.199 2(4)	Mn(2)-N(7)	0.244 2(5)	Mn(6)-Na(1)	0.342 6(2)
Mn(1)-O(24)	0.218 0(4)	Mn(2)-Mn(4)	0.317 25(11)	Mn(5)-O(14)	0.218 2(4)
Mn(1)-N(8)	0.236 0(5)	Mn(2)-Na(2)	0.347 4(2)	Mn(5)-O(26)	0.218 8(4)
Mn(1)-Mn(4)	0.314 86(12)	Mn(6)-O(11)	0.187 3(3)	Mn(5)-O(28)	0.220 5(3)
Mn(1)-Na(2)	0.340 8(2)	Mn(6)-O(28)	0.188 5(3)	Mn(5)-O(15)	0.220 4(3)
Mn(2)-O(17)	0.188 0(3)	Mn(6)-O(8)	0.191 6(3)		
Mn(2)-O(15)	0.188 7(3)	Mn(6)-N(17)	0.198 0(4)		
O(17)-Mn(1)-O(16)	92.99(15)	O(16)-Mn(1)-O(18)	174.02(16)	O(16)-Mn(1)-N(22)	83.68(16)
O(17)-Mn(1)-O(18)	92.98(15)	O(17)-Mn(1)-N(22)	168.27(17)	O(18)-Mn(1)-N(22)	90.38(16)

Continued Table 2

2					
Mn(1)-O(15)	0.187 9(2)	Mn(2)-O(10)	0.187 0(2)	Mn(3)-N(6)	0.197 6(3)
Mn(1)-O(10)	0.187 9(2)	Mn(2)-O(9)	0.188 9(2)	Mn(3)-N(3)	0.225 1(4)
Mn(1)-O(13)	0.191 1(2)	Mn(2)-O(6)	0.199 5(3)	Mn(3)-N(4)	0.238 8(3)
Mn(1)-N(7)	0.198 3(3)	Mn(2)-O(4)	0.214 3(3)	Mn(3)-Na(1)	0.342 10(15)
Mn(1)-O(5)	0.215 9(3)	Mn(2)-Mn(3)	0.323 54(7)	Mn(4)-O(7)	0.217 2(2)
Mn(1)-N(4)	0.252 4(3)	Mn(2)-Na(1)	0.344 78(15)	Mn(4)-O(8)	0.217 9(2)
Mn(1)-Mn(3)	0.318 36(7)	Mn(3)-O(8)	0.190 1(2)	Mn(4)-O(15)	0.226 0(2)
Mn(1)-Na(1)	0.344 89(15)	Mn(3)-O(11)	0.190 2(2)		
Mn(2)-O(7)	0.187 0(2)	Mn(3)-O(10)	0.191 0(2)		
O(15)-Mn(1)-O(10)	92.83(10)	O(15)-Mn(1)-O(5)	92.16(11)	O(13)-Mn(1)-N(7)	90.58(12)
O(15)-Mn(1)-O(13)	173.78(10)	O(15)-Mn(1)-N(7)	84.02(12)		
O(10)-Mn(1)-O(13)	91.67(10)	O(10)-Mn(1)-N(7)	165.93(12)		

2 Results and discussion

2.1 Structure description

Complex **1** crystallizes in the monoclinic system, while **2** crystallizes in the triclinic system with the similar structure. Herein, the molecular structure of complex **1** is described in detail as a representative example. As shown in Fig.1, complex **1** consists of seven Mn ions, two Na^+ ions, six L^{2-} ions, four N_3^- anions and four DMF solvent molecules. The two peripheral $[Mn^{Ⅲ}{}_3O]^{7+}$ triangles are each bonded to a central Mn^{2+} ion. This ion is linked to each triangle via the O atom of the ligand. The Mn ions in each triangle are linked to each other via one μ_4-O^{2-} ion, one η^1:η^1:μ-acetates, and the two N_3^- groups via the N atoms to form a $[Mn^{Ⅲ}{}_6Mn^{Ⅱ}(\mu_4\text{-}O^{2-})_2(\mu\text{-}OOCCH_3)_2(\mu\text{-}N_3)_4]^{10+}$ core. The Na^+ ion links to the Mn via three O atoms of three L^{2-} ligands. The central μ_4-O atom deviates 0.222 nm from the mean plane formed by three Mn ions, which is similar with the reported structure[7a]. The angle of Mn-N(N_3)-Mn is 83.20° and 85.65°, respectively. The average distance between Na^+ ion and μ_4-O is 0.267 7 nm. The average angle of Mn-O-Mn is 106.76°. The structure of **2** is similar with **1**, except that the SCN group replaces the N_3 group. The central μ_4-O deviates 0.018 3 nm from the mean plane formed by three Mn ions, which is similar with **1**. The angle of Mn-N(NCS)-Mn is 80.73° and 80.06°, respectively. The distance

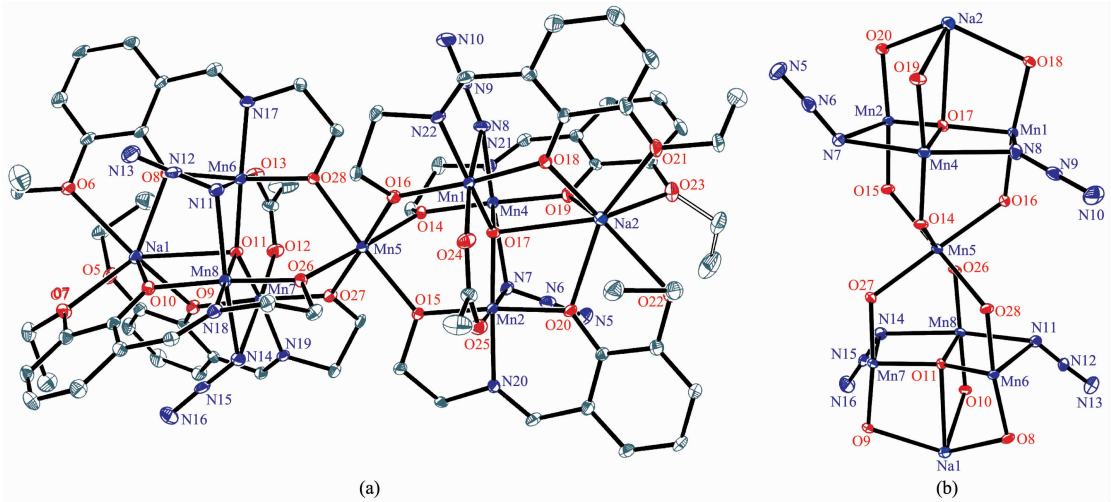

H atoms have been omitted for clarity

Fig.1 Molecular structure (a) and coordination environment (b) of complex **1** with 40% probability displacement ellipsoids

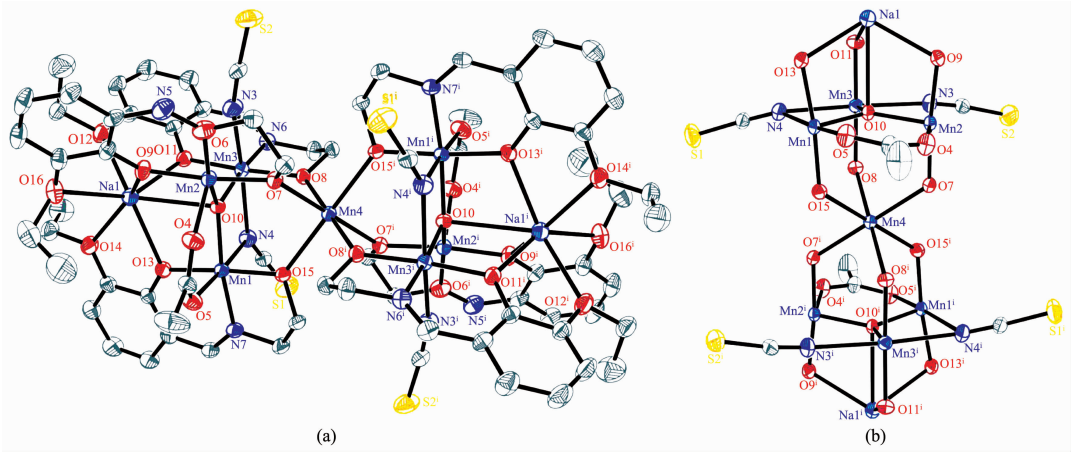

H atoms have been omitted for clarity; Symmetry codes: ^{i} $-x+1, -y, -z+1$

Fig.2 Molecular structure (a) and coordination environment(b) of complex **2** with 40% probability displacement ellipsoids

between Na^+ ion and μ_4-O is 0.270 0 nm. The average angle of Mn-O-Mn is 108.13°.

2.2 X-ray powder diffraction analyses

Complexes **1** and **2** were also characterized by powder X-ray diffraction (PXRD) at room temperature. The patterns calculated from the single-crystal X-ray data of **1** and **2** were in good agreement with the observed ones in almost identical peak positions (Fig. 3). The difference in reflection intensities between the simulated and experimental patterns was due to the powder size and variation in preferred orientation for the powder samples during collection of the experimental PXRD data.

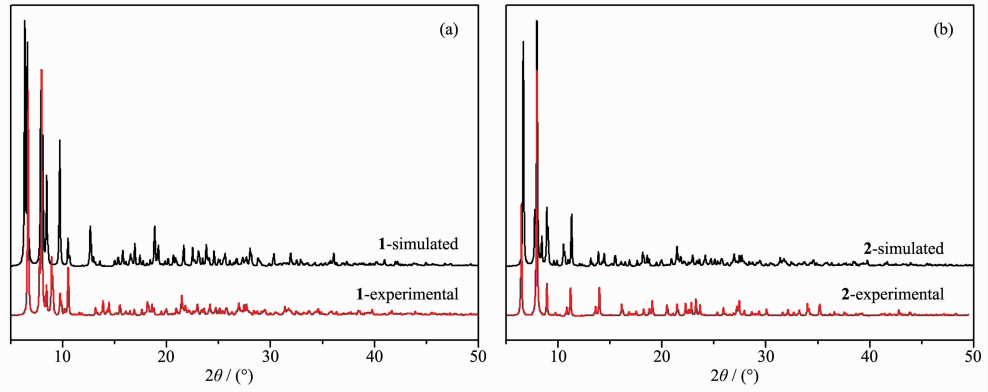

Fig.3　XRD patterns of complex **1** (a) and **2** (b)

2.3 Thermal stability

Thermal stability is an important aspect for the application of coordination compound. Thermogravimetric analysis (TGA) experiments were carried out to determine the thermal stabilities of **1** and **2** (Fig.4). For complex **1**, there are many solvent molecules in the structure, and TG curves showed the first consecutive step of weight loss that was observed in a range of 40~250 ℃, corresponding to the release of solvent molecules. Then, the continuously weight loss corresponds to the loss of ligands (in the range of 180~750 ℃). Finally, the weight loss ended until

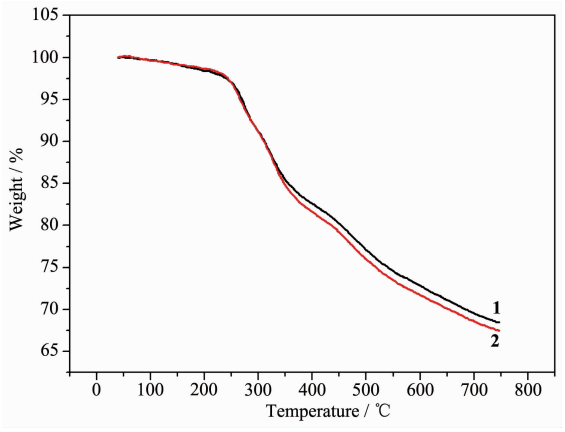

Fig.4　TGA curves of complexes **1** and **2**

heating to 750 ℃ and the total weight loss was about 68%. For **2**, TG curves was similar with complex **1**, the weight loss ended until heating to 750 ℃ and the total weight loss was about 67%.

2.4 Magnetic studies

The variable-temperature dc magnetic susceptibility measurement for complexes **1** and **2** were performed in the temperature range of 2~300 K under an applied magnetic field of 1 000 Oe. The collected data are plotted as $\chi_M T$ vs T in Fig.5 and Fig.6. The $\chi_M T$ value at room temperature of complex **1** was 26.13 $cm^3 \cdot mol^{-1} \cdot K$, which is higher than the theoretically predicted value (22.37 $cm^3 \cdot mol^{-1} \cdot K$) for six Mn^{3+} and one Mn^{2+} ions[14]. With the temperature decreasing, the $\chi_M T$ product of **1** decreased until 8.5 K, and then increased rapidly to 9.89 $cm^3 \cdot K \cdot mol^{-1}$ at 2 K, suggesting the presence of intramolecular ferromagnetic coupling between the Mn^{3+} and Mn^{2+} for **1** below 8.5 K[15]. The temperature dependence of the reciprocal susceptibility χ_M^{-1} values at high temperature were fitted by the Curie-Weiss law, $\chi_M = C/(T-\theta)$, with C = 21.50 $cm^3 \cdot mol^{-1} \cdot K$ and θ=−59.09 K. The negative θ values confirm antiferromagnetic coupling among metal centers of **1**. For complex **2**, the $\chi_M T$ product at 300 K are 16.14 $cm^3 \cdot mol^{-1} \cdot K$, which is lower than the theoretically predicted value for six Mn^{3+} and one Mn^{2+} ions. As the temperature decreasing, $\chi_M T$ values gradually decreased, then underwent a rapid decrease until to 2.09 $cm^3 \cdot mol^{-1} \cdot K$ at 2 K, indicating the presence of intramolecular antiferromagnetic interactions between the Mn^{3+} and Mn^{2+} ions. The temperature dependence of the reciprocal susceptibility χ_M^{-1} values above 50 K were fitted by the Curie-Weiss law with the obtained constant C=21.90 $cm^3 \cdot mol^{-1} \cdot K$ and θ=−103.71 K. The negative value of θ confirms an antiferromagnetic coupling among metal centers of **2**.

To explore the dynamic magnetic property of the complexes, the temperature dependence of the alternating-current (ac) magnetic susceptibility for **1** and **2** under a zero direct-current (dc) magnetic field

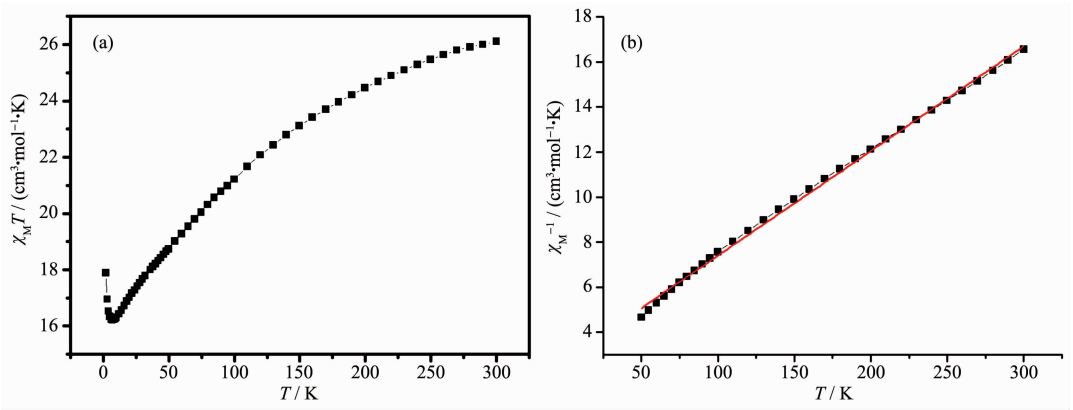

Fig.5 Temperature dependence of $\chi_M T$ at 1 000 Oe (a) and $1/\chi_M$ vs T plot (b) for **1**

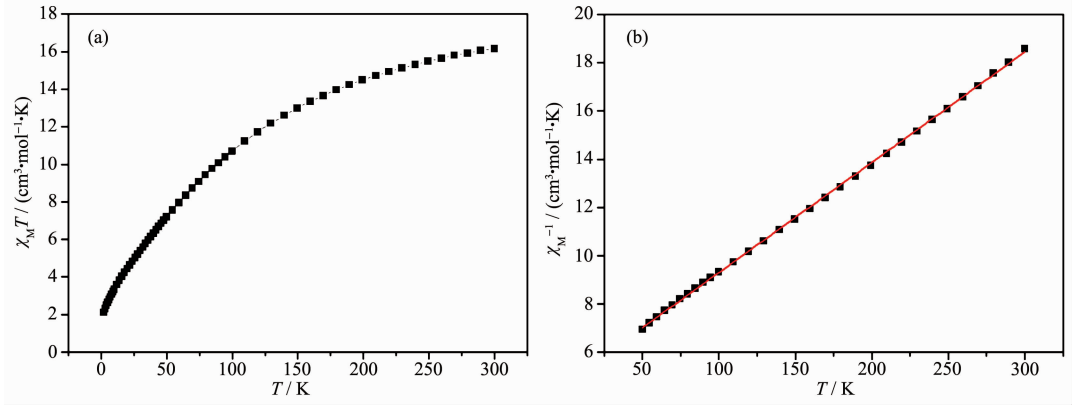

Fig.6 Temperature dependence of $\chi_M T$ at 1 000 Oe (a) and $1/\chi_M$ vs T plot (b) for **2**

oscillating at 1~320 Hz was recorded in Fig.7 and Fig.8. As can be seen, **1** and **2** didn′t exhibit the frequency-dependent character in out-of-phase (χ'') signals and in-phase (χ') signals. The result shows that the complexes **1** and **2** are not single molecule magnet (SMM).

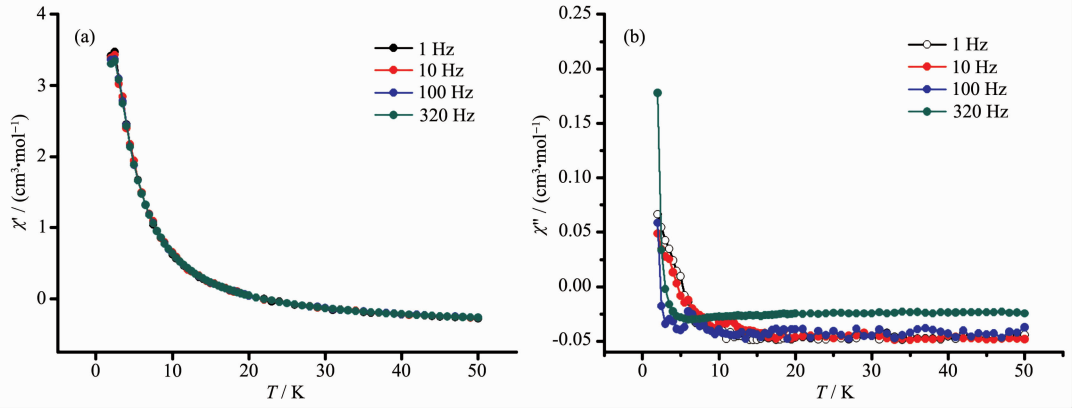

Fig.7　Plots for temperature dependence of in-phase (χ') (a) and out-of-phase (χ'') (b) ac susceptibility for **1** under zero applied dc magnetic field

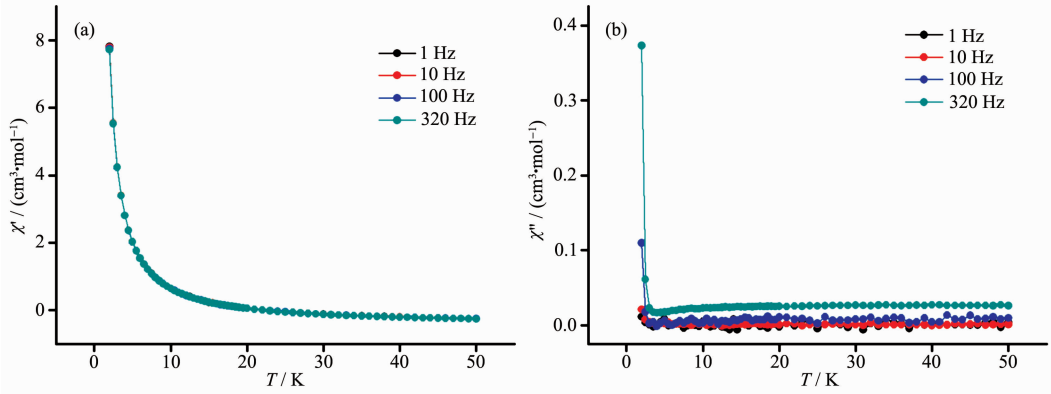

Fig.8　Plots for temperature dependence of in-phase (χ') (a) and out-of-phase (χ'') (b) ac susceptibility for **2** under zero applied dc magnetic field

3　Conclusions

In summary, two new manganese complexes with Schiff-base ligands were synthesized and characterized by elemental analysis, IR spectra, thermogravimetric analyses and single crystal X-ray diffraction analysis. The investigation of magnetic studies confirms the antiferromagnetic interactions between the Mn^{2+} and Mn^{3+} ions for complexes **1** and **2**. Furthermore, the dynamic magnetic property of the complexes **1** and **2** was studied, and it is found that the complexes **1** and **2** are not SMM.

References:

[1] Caneschi A, Gatteschi D, Sessoli R. *J. Chem. Soc. Dalton Trans.*, **1997**(21):3963-3970

[2] Wieghardt K. *Angew. Chem. Int. Ed.*, **1994**,**33**(7):725-728

[3] Thomas L, Lionti F L, Ballou R, et al. *Nature*, **1996**,**383**(6596):145-147

[4] Squire R C, Aubin S M J, Folting K, et al. *Inorg. Chem.*, **1995**,**34**(26):6463-6471

[5] Bhula R, Weatherburn D C. *Angew. Chem. Int. Ed.*, **1991**,**30**(6):688-689

[6] Goldberg D P, Caneschi A, Delfs C D, et al. *J. Am. Chem. Soc.*, **1995**,**117**(21):5789-5800

[7] (a)XU Min(徐敏), ZHOU Ai-Ju(周爱菊), LI Dong-Xiang(李东香), et al. *Chinese J. Inorg. Chem.*(无机化学学报), **2013**,**29**(4):826-830

(b)Murugesu M, Wernsdorfer W, Abboud K A, et al. *Angew. Chem.*, **2005**,**117**(6):914-918

[8] (a)Milios C J, Vinslava A, Wernsdorfer W, et al. *J. Am. Chem. Soc.*, **2007**,**129**(10):2754-2755

(b)Yang C I, Wernsdorfer W, Lee G H, et al. *J. Am. Chem. Soc.*, **2007**,**129**(3):456-457

(c)Milios C J, Inglis R, Bagai R, et al. *Chem. Commun.*, **2007**(33):3476-3478

(d)Milios C J, Inglis R, Vinslava A, et al. *J. Am. Chem. Soc.*, **2007**,**129**(41):12505-12511

[9] (a)Brechin E K, Soler M, Christou G, et al. *Chem. Commun.*, **2003**(11):1276-1277

(b)Milios C J, Fabbiani F P A, Parsons S, et al. *Dalton Trans.*, **2006**(2):351-356

[10] (a)Dendrinou-Samara C, Zaleski C M, Evagorou A, et al. *Chem. Commun.*, **2003**(21):2668-2669

(b)Boskovic C, Brechin E K, Streib W E, et al. *Chem. Commun.*, **2001**(5):467-468

[11]Wu L J, Yang H, Zeng S Y, et al. *Polyhedron*, **2017**,**129**:77-81

[12]Sheldrick G M. *SADABS* 2.05, University of Göttingen, **2000**.

[13]Sheldrick G M. *SHELXL Reference Manual, Ver.*5.1, Madison, WI, Bruker Q16 Analytical X-Ray Systems, **1997**.

[14]Milios C J, Gass I A, Vinslava A, et al. *Inorg. Chem.*, **2007**, **46**(16):6215-6217

[15]Cao F, Wei R M, Li J, et al. *Inorg. Chem.*, **2016**,**55**(12):5914-5923